scientific reports

Check for updates

OPEN

Intratumoral microbiota as a novel prognostic indicator in bladder cancer

Yuwei Zhang[1,2,5], Hao Lin[2,3,5], Linghui Liang[2,3,5], Shengkai Jin[2], Jing Lv[2], Yuhua Zhou[2], Feng Xu[4]✉, Fengping Liu[2]✉ & Ninghan Feng[1,2,3]✉

Microbes are important components of the tumor microenvironment and have a close relationship with tumors. However, there is still a lack of research on the intratumoral microbiota in bladder cancer and its impact on the tumor immune microenvironment. In this study, we used fluorescence in situ hybridization (FISH) and observed a substantial presence of microbiota in bladder cancer tissues, with greater abundance compared to that in normal bladder tissues. Based on the BIC database, we found that the microbiome of bladder cancer is highly diverse and its structure is significantly different from that of other tumors. To investigate the relationships among the intratumoral microbiota, tumor immunity, and prognosis in bladder cancer patients, we analyzed bladder cancer-specific differentially expressed immune- and antimicrobial-related genes from the ImmPort, TISIDB, and TCGA databases. We identified 11 hub genes and constructed a prognostic risk model. Further analysis revealed differences at the family and genus levels between distinct groups. Using LEfSe analysis, we identified six hub biomarkers and developed a novel microbial-based scoring system. The scoring system allows subgrouping of bladder cancer patients, with significant differences in prognosis, immune cell infiltration, tumor mutation burden, and immune checkpoints among different groups. Further FISH and immunofluorescence co-staining experiments initially verified that the specific distribution of microorganisms and M2 macrophages in bladder cancer may be closely related to the poor prognosis of patients. In conclusion, this study revealed the characteristics of the intratumoral microbiota in bladder cancer and identified potential prognostic targets for clinical application.

Keywords Intratumoral microbiota, Bladder cancer, Tumor immune microenvironment, Bacteria in cancer, Prognostic indicator

Abbreviations

ETBF	Enterotoxigenic *Bacteroides fragilis*
ROS	Reactive oxygen species
ICI	Immune checkpoint inhibitors
TIME	Tumor immune microenvironment
MSI	Microsatellite instability
MS	Microbial-based scoring
FISH	Fluorescence in situ hybridization
TMB	Tumor mutation burden
TCGA	The Cancer Genome Atlas
ImmPort	The immunology database and analysis portal
TISIDB	The tumor immune system interactions database
BIC	The bacteria in cancer
IF	Immunofluorescence
FDR	False discovery rate
K-M	Kaplan-Meier
ROC	Receiver operating characteristic

[1]Medical School of Nantong University, 9 Qiangyuan Road, Nantong 226019, China. [2]Department of Urology, Jiangnan University Medical Center, No. 1800, Lihu Avenue, Wuxi 214122, China. [3]Department of Urology, Wuxi No.2 Hospital, Nanjing Medical University, Wuxi, China. [4]Department of Urology, Jinling Hospital, Affiliated Hospital of Medical School, Nanjing University, 22 Hankou Road, Nanjing 210093, China. [5]Yuwei Zhang, Hao Lin and Linghui Liang contributed equally to this work. ✉email: msn1999@sina.com; liulaoshiyc@163.com; n.feng@njmu.edu.cn

STAMP The statistical analysis of metagenomic profiles

Bacteria, archaea, and viruses, along with their genomes and products, are widely present in the human body, with the gut microbiome being the most prominent[1]. The gut microbiota is closely associated with human health, and disruption of its stability can lead to the occurrence and progression of various diseases. For instance, studies have shown that patients with Crohn's disease have a significantly decreased abundance of *Faecalibacterium prausnitzii* in their feces, which is closely associated with disease relapse[2]. Previous studies have reported that enterotoxigenic *Bacteroides fragilis* (ETBF) is present in more than 80% of colorectal cancer patients. ETBF colonizes the colon mucosa and continuously produces enterotoxins, promoting the development of disease by causing DNA damage in host cells through increased levels of reactive oxygen species (ROS)[3]. Previous studies have focused primarily on the gut microbiome in human microbiome research. However, with advancements in microbial research and the emergence of high-throughput sequencing technologies, it has been discovered that many tissues previously believed to be sterile actually harbor microorganisms. The microbiota in tissues such as the lung, prostate, bladder, breast, liver, and pancreas has been found to be closely associated with various physiological and pathological processes[4]. Interestingly, recent studies have indicated the presence of microorganisms within tumors, including bacterial communities within tumor cells and the tumor microenvironment[5]. In particular, various anaerobic or facultative anaerobic bacteria have been detected in necrotic areas within breast tumor tissues[6]. Through research on the microbiome, new insights into diseases such as tumors have been gained.

Previous studies have shown that microorganisms within tumors can exploit the immune escape capacity of tumors to evade clearance by the immune system[7]. Some microorganisms or their metabolites are also involved in the development of tumors. For example, *Fusobacterium nucleatum* has been reported to play an important role in the recruitment, differentiation and proliferation of intratumoral immune cells in patients with colorectal cancer[8]. In addition, the efficacy of immune checkpoint inhibitors (ICIs) in patients with *Gostriidium* in the tumor was better than that in patients with *Raginalis* in the tumor[9]. Some microbial metabolites that accumulate in tumors, such as fatty acids and adenosine, have also been shown to bind to key receptors on cancer cells and immune cells[10–12]. In summary, the intratumoral microbiome has the potential to change the tumor immune microenvironment (TIME), thereby affecting tumor development.

The tumor microbiome varies greatly from patient to patient, making it an attractive target for personalized disease prediction and treatment. For example, studies have shown that the tumor microbiome of pancreatic cancer patients who have prolonged survival has greater alpha diversity[13]. In addition, the tumor microbiome is also closely related to patient immunotherapy efficacy. Previous studies have shown that the effect of immunotherapy in patients with colorectal cancer is closely related to carcinogenic microorganisms such as *F. nucleatum* and *Colicinogeny*[14,15]. Further studies have shown that the DNA load of *F. nucleatum* in colorectal cancer patients with high microsatellite instability (MSI) is negatively correlated with the density of tumor-infiltrated FoxP3 T cells but is positively correlated with the proportion of M2 macrophages[16]. Therefore, the intratumoral microbiome is closely related to the infiltration of immune cells in the tumor microenvironment.

Bladder cancer is a prevalent malignant tumor of the urinary system and ranks fourth among male malignant tumors in European and American countries[17]. During diagnosis, urothelial carcinoma of the urinary tract is classified as non-muscle-invasive bladder cancer (NMIBC) or muscle-invasive bladder cancer (MIBC). The treatment approaches for different subtypes vary significantly. With molecular pathology playing a leading role in diagnosis, treatment selection, and follow-up planning, the importance of biomarkers in disease management will further increase. The most commonly utilized molecular markers to date are genetic variations in TP53, ERCC1, and FGFR3, which can serve as indicators of disease progression, chemotherapy sensitivity, and small molecule treatment selection[18]. However, the discovery and validation of other biomarkers remain crucial. Smoking is often considered one of the major risk factors for bladder cancer. However, it is worth considering that with the obvious increase in the proportion of female smokers, the incidence of female bladder cancer has not increased significantly[19]; therefore, other important factors may be affecting the occurrence and development of bladder cancer. Recent studies have revealed a close relationship between the urinary microbiota and bladder cancer, suggesting that microbiota could serve as a biomarker and a valuable therapeutic target[20]. However, there is still a lack of research on whether the microbiota in bladder cancer patients undergoes changes and whether these changes are associated with the occurrence and progression of the disease.

The BIC database was the first to include TCGA miRNA sequencing data, which was used to analyze bacterial abundance and transcription landscape across 32 types of cancers[21]. The BIC database revealed that bladder cancer tissues have a high abundance of microbiota, and subsequent analyses revealed that microbiota were specifically associated with bladder cancer. Additionally, we developed a microbial-based scoring (MS) system and explored the relationships between the MS system and patient survival outcomes, immune infiltration, and immune checkpoints.

Results

Presence of intratumoral microbiota in BLCA

The flowchart of the present study is shown in Fig. 1. To investigate the presence of microbiota in bladder cancer, we employed fluorescence in situ hybridization (FISH) using the EUB338 probe in both bladder cancer tissues and adjacent normal tissues (Fig. 2A,B). Signal detection via FISH confirmed the presence of bacteria in both bladder cancer and adjacent normal tissues. Importantly, the intratumoral microbiota in bladder cancer tissues was significantly greater than that in normal bladder tissues. Furthermore, we explored the relationship between intratumoral microbiota and immune cells in bladder cancer. The results indicated a lower distribution of CD8+ cells (Fig. 2C) and a greater distribution of macrophages in bladder cancer tissues (Fig. 2D). Interestingly, regions with a greater abundance of macrophages exhibited a significant reduction in intratumoral microbiota.

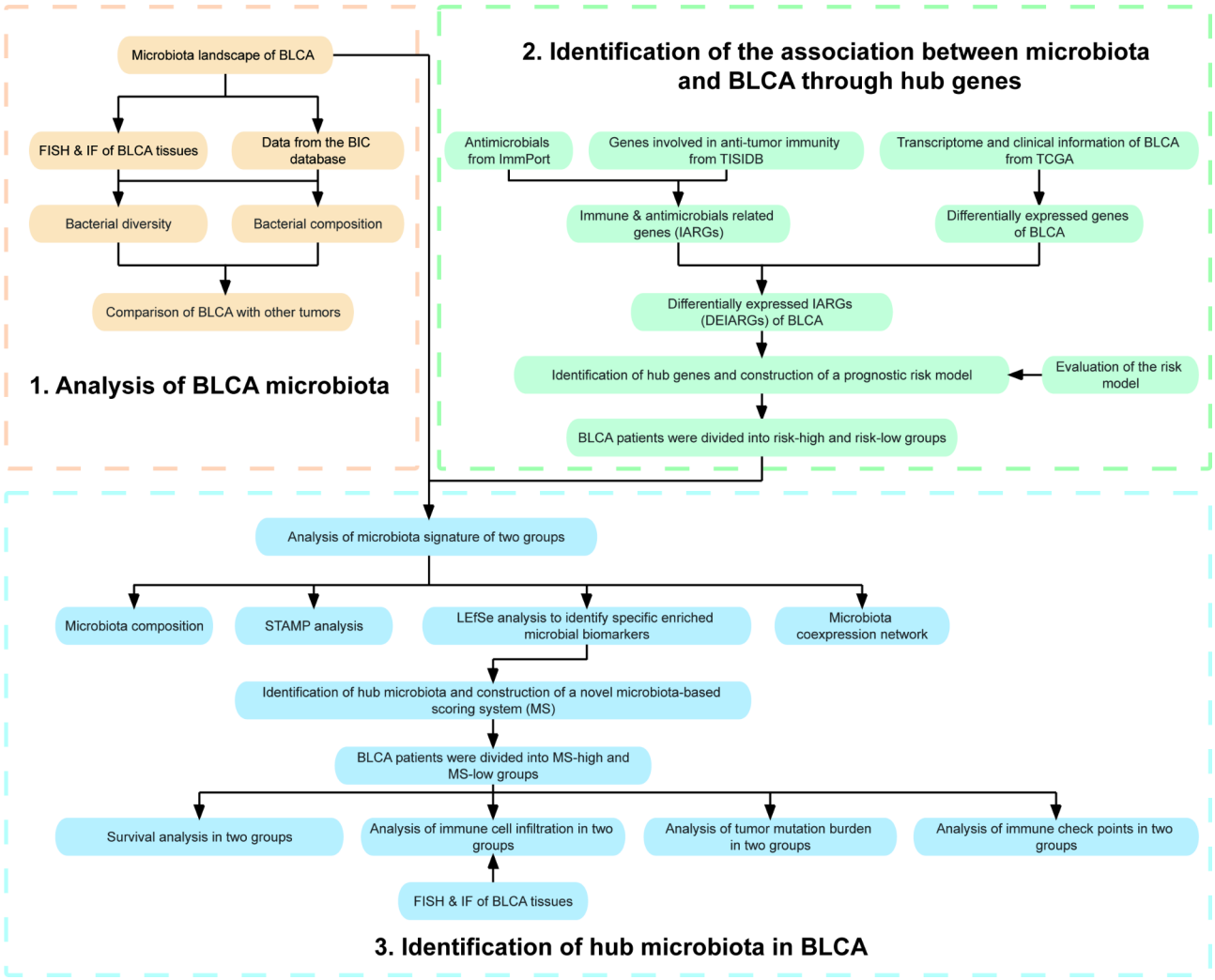

Fig. 1. The flowchart of this study. The whole study is divided into three parts. Firstly, we conducted an overall analysis of the intratumoral microbiota in BLCA, including the bacteria composition and abundance. Then, we managed to divide BLCA patients into the high-risk and low-risk groups based on the Immune & antimicrobials related genes in BLCA. Finally, we identified key intratumoral microbiota in BLCA patients that could serve as biomarkers, and based on this, we constructed a novel microbial-based scoring system.

The phenotype and function of macrophages are regulated by the surrounding microenvironment, namely, the phenomenon of macrophage polarization. Polarized macrophages, which can be divided into M1 and M2 types, play a crucial role in regulating tumor progression, metastasis, and clinical outcome. Among them, M2 macrophages have been reported to promote the occurrence and progression of tumors[22]. We conducted FISH and IF experiments in bladder cancer tissues. The results showed that the infiltrating macrophages in bladder cancer were mainly M2 macrophages (Fig. 2E) rather than M1 macrophages (Fig. 2F).

Landscape of the BLCA microbiota

We analyzed the bacterial diversity at the genus level across cancers in the BIC database. The BLCA Shannon index ranked 11th out of 32 tumors (full name is shown in Supplementary Table 1), indicating high bacterial diversity in BLCA (Fig. 3A). Subsequently, we analyzed the microbiota composition of BLCA. The top ten bacteria at the genus level were *Paenibacillus*, *Pseudomonas*, *Bacillus*, *Peptoclostridium*, *Acinetobacter*, *Brevibacillus*, *Corynebacterium*, *Prevotella*, *Azotobacter* and *Actinoplanes* (Fig. 3B).

The structure of the intratumoral microbiota across cancers is specific. We compared the top 10 intratumoral bacteria in BLCA and colorectal carcinomas, and the Venn diagram showed that only three microorganisms at the genus level overlapped, namely, *Pseudomonas*, *Bacillus* and *Prevotella* (Fig. 3C). We then compared BLCA with other urological tumors, including three different types of kidney cancer. Interestingly, the microbial structure of BLCA is similar to that of other urological cancers. The top ten intratumoral bacteria of BLCA overlapped 7 with KIRC (*Paenibacillus*, *Pseudomonas*, *Bacillus*, *Acinetobacter*, *Brevibacillus*, *Corynebacterium*, and *Azotobacter*), 7 with KIRP (*Paenibacillus*, *Pseudomonas*, *Bacillus*, *Acinetobacter*, *Brevibacillus*, *Corynebacterium*, and *Actinoplanes*), 5 with KICH (*Pseudomonas*, *Acinetobacter*, *Corynebacterium*, *Azotobacter*, and *Actinoplanes*),

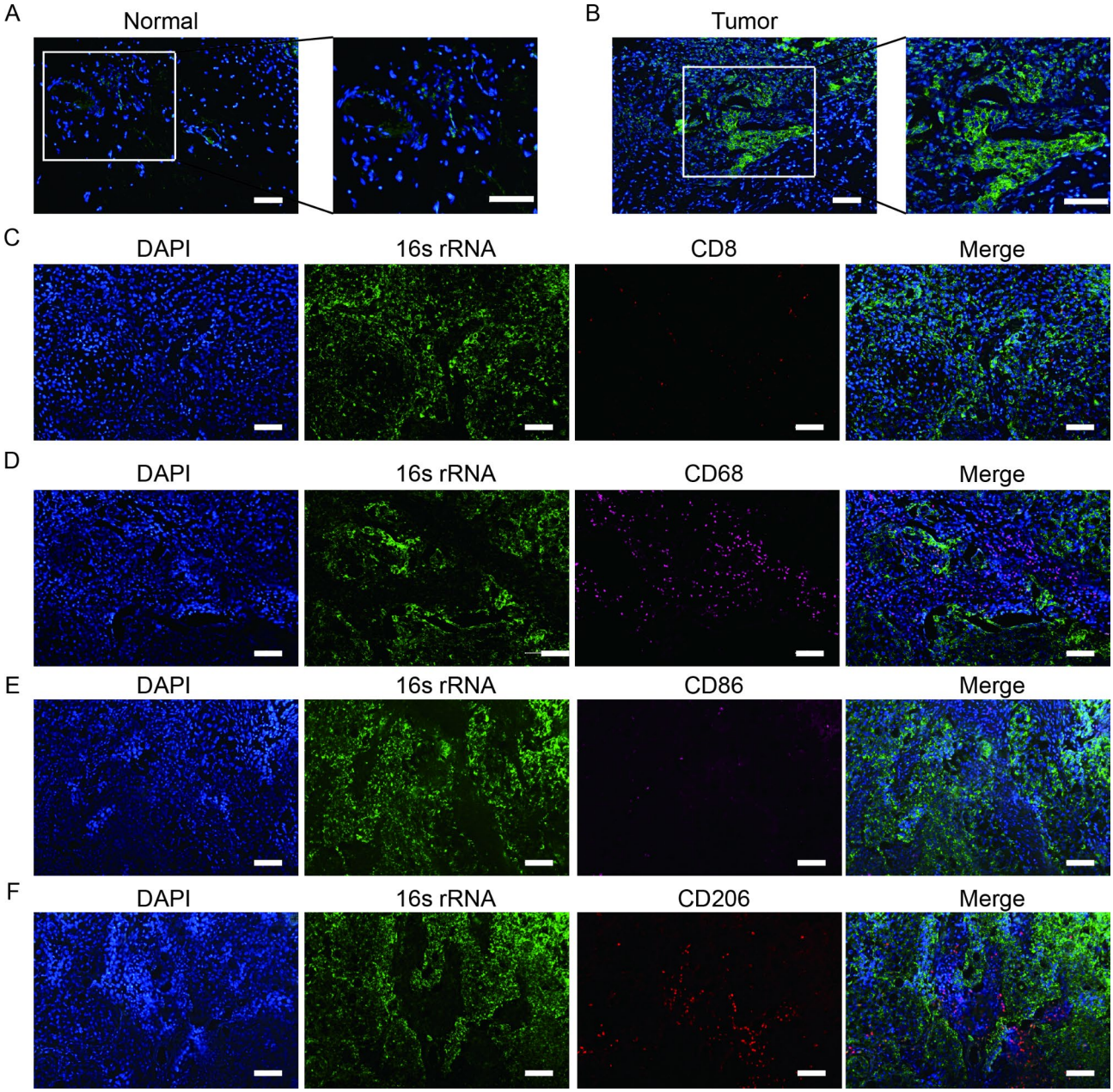

Fig. 2. Presence of intratumoral microbiota and staining of immune cells in bladder cancer tissues. (**A**, **B**) Fluorescence in situ hybridization (FISH) analysis of bacterial 16 S rRNA in normal bladder tissue (**A**) and bladder cancer tissue (**B**) stained with the EUB338 probe (green) and DAPI (blue). (**C**, **D**) Co-staining of immune cells and bacterial 16 S rRNA in bladder cancer tissue. CD8+ T cells are marked in red (**C**), while macrophages are marked in pink (**D**). (**E**, **F**) Co-staining of immune cells and bacterial 16 S rRNA in bladder cancer tissues. M1 macrophages are marked in pink (**E**), while M2 macrophages are marked in red (**F**). Scale bar = 100 μm.

and even 8 with PRAD (*Paenibacillus*, *Pseudomonas*, *Bacillus*, *Peptoclostridium*, *Acinetobacter*, *Brevibacillus*, *Corynebacterium*, amd *Azotobacter*). A total of three microorganisms, namely, *Pseudomonas*, *Acinetobacter* and *Corynebacterium*, were among the top 10 in bacteria abundance in all five tumors (Fig. 3D).

The intratumoral microbiota structure of urogenital system cancers exhibits a high degree of similarity, which may be related to the proximity of anatomical locations and the influence of the urinary microbiome.

Construction of a prognostic risk model for BLCA based on differentially expressed immune- and antimicrobial-related genes (DEIARGs)

We downloaded a list of antimicrobial-related genes from the ImmPort database and a list of tumor immune-related genes from the TISIDB (Supplementary Table 2). The combination of these two gene lists revealed 1330 genes, which are referred to as immune- and antimicrobial-related genes (IARGs) (Fig. 4A). We identified 4840

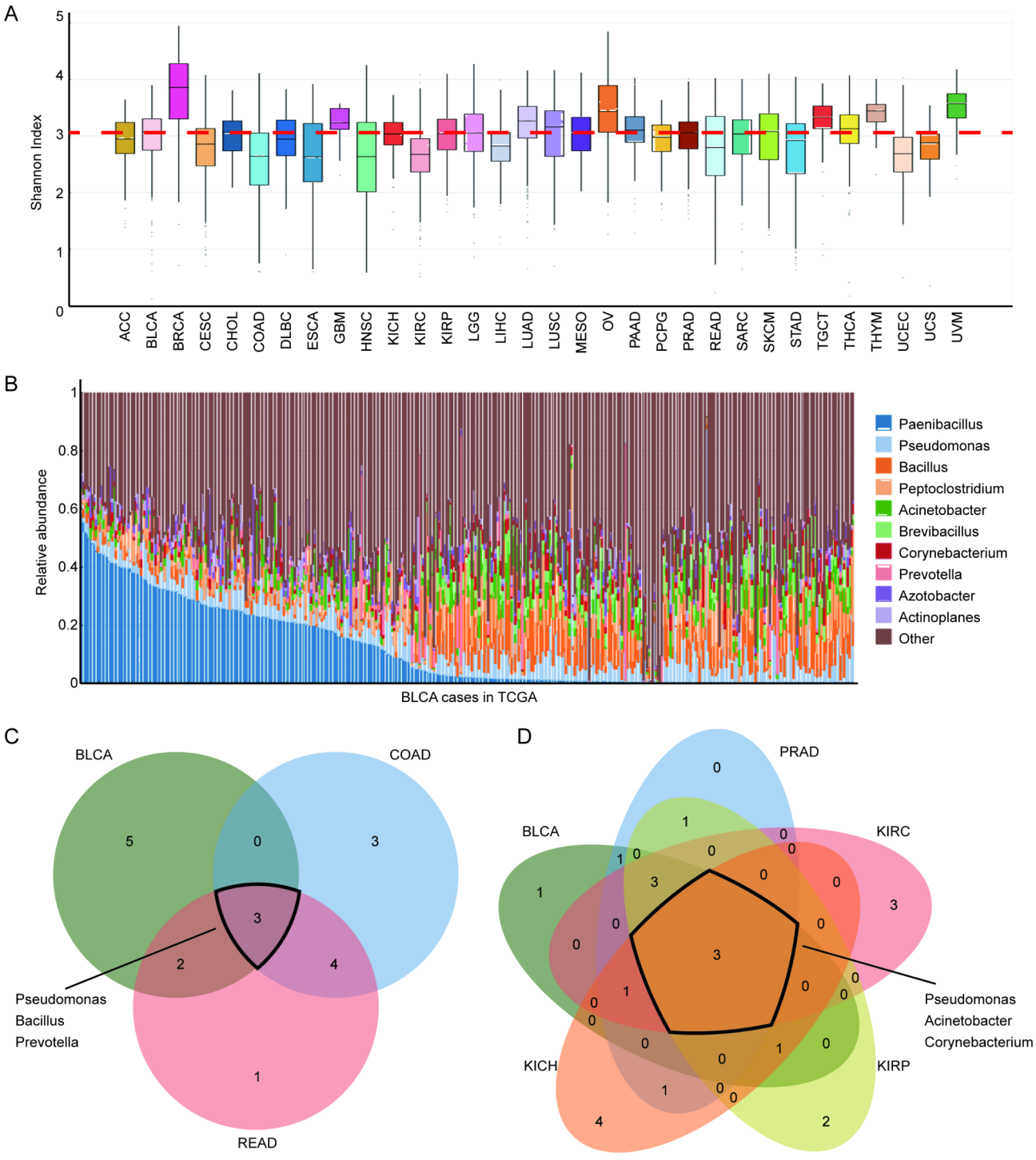

Fig. 3. Landscape of BLCA microbiota. (**A**) Bacterial diversity at the genus level across cancers. The red line indicates the mean diversity index of BLCA. (**B**) Stacked bar plot of the bacterial composition detected in BLCA patients. The bar plot shows the relative abundances of the top ten bacteria at the genus level. (**C**) The Venn diagram displays the overlap of the top ten genera in terms of relative abundance in BLCA and colorectal carcinomas. (**D**) The Venn diagram displays the overlap of the top ten genera in terms of relative abundance in BLCA and other urological tumors.

differentially expressed genes (DEGs) from the transcriptome data of TCGA bladder cancer and normal bladder tissue samples. By comparing this gene list with those of IARGs, we ultimately obtained 331 DEIARGs (Fig. 4B, Supplementary Table 3).

To construct a DEIARG-based prognostic model for BLCA patients, we first performed univariate Cox regression analysis, and a total of 34 genes were screened (Supplementary Fig. 1). Then, LASSO Cox regression

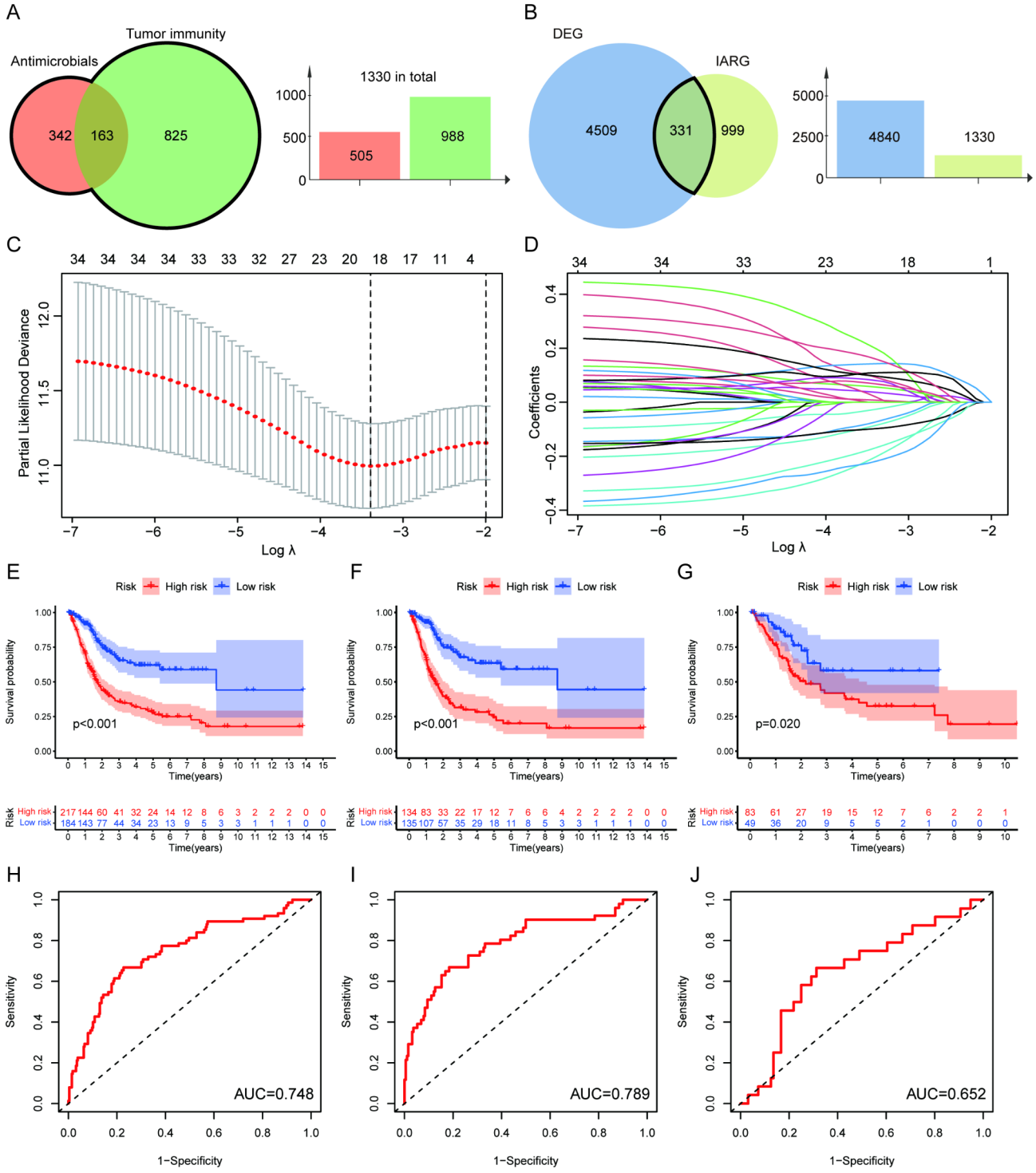

Fig. 4. Construction of a prognostic risk model of BLCA based on DEIARGs. (**A**) A total of 1330 genes were identified as immune- and antimicrobial-related genes (IARGs). (**B**) Venn diagram shows 331 genes identified as differentially expressed IARGs (DEIARGs) in BLCA. (**C, D**) LASSO Cox regression analysis of DEIARGs. (**E, G**) K-M curves of the All dataset, training group and testing group. (**H**-**J**) ROC curves of the All dataset, training group and testing group.

analysis and multivariate Cox regression analysis were conducted (Fig. 4C,D), and the 11 hub genes that were most significantly associated with the prognosis of BLCA patients were ultimately identified (Supplementary Table 4). Patients with bladder cancer were randomly divided into a training group ($n=269$) and a testing group ($n=132$) to construct and validate prognostic risk models (Supplementary Table 5). Analysis of patient characteristics in the training group and the testing group showed good similarity between the two groups

(Supplementary Table 6). All patients were further divided into high-risk and low-risk groups based on the median risk score obtained from the training group. K-M survival curves (Fig. 4E-G) and ROC curves (Fig. 4H-J) show the reliability of the prognostic risk model. Patients with higher risk scores had shorter overall survival and worse prognosis.

We further visualized the expression of the 11 hub genes to better visualize the differential expression of these genes between the high-risk and low-risk groups (Supplementary Fig. 2A-C). Overall, our risk model showed that patients with higher risk scores had worse outcomes, while patients with lower risk scores had better outcomes (Supplementary Fig. 2D-I). In addition, using the Metascape database (https://Metascape.org/gp/index.html#/main/step1), a Gene Annotation & Analysis Resource, we conducted an analysis of the 11 hub genes. Pathway and process enrichment analyses were performed using various ontology sources, including KEGG Pathway[23], GO Biological Processes, Reactome Gene Sets, Canonical Pathways, CORUM, WikiPathways, and PANTHER Pathway. These hub genes are closely related to various tumor diseases and processes (Supplementary Fig. 2J and Supplementary Tables 7–8).

Differential microbiota signatures in the high-risk and low-risk groups

To investigate the differences in the bladder microbiota between high-risk and low-risk patients, we conducted a series of analyses. First, we analyzed the alpha and beta diversity of the intratumoral microbiota in the high-risk and low-risk groups. No significant difference in the alpha or beta diversity was observed between the two groups at the phylum (Supplementary Fig. 3A, C) or genus levels (Supplementary Fig. 3B, D).

To visualize the differences in the composition of the microbiota between the two groups, we identified the top 10 most abundant microbes at different taxonomic levels (Fig. 5A-E). No significant differences were observed between the two groups at the phylum, class and order levels. However, at the family and genus levels, the microbial compositions of the two groups were significantly different. In particular, the abundance of *Sanguibacter*, *Elizabethkingia*, *Actinobacillus* and *Spirochaeta* in the low-risk group was significantly greater than that in the high-risk group. Whether these bacteria are beneficial to the prognosis of BLCA patients deserves further study.

Then, we used statistical analysis of metagenomic profiles (STAMP) to specifically analyze the different microorganisms between the high-risk and low-risk groups. Overall, 2, 4, 4, 6, and 15 distinct microorganisms were found between the two groups at the phylum, class, order, family, and genus levels, respectively (Fig. 5F-J).

At the phylum level, the abundance of Aquificae was much greater in the high-risk patients than in the low-risk patients, while Chlamydiae showed the opposite trend. At the genus level, *Pseudoalteromonas*, *Thermocrinis*, *Amycolatopsis*, *Sanguibacter*, and *Spirochaeta* were the most significantly different bacteria between the two groups.

Microbiota co-expression network in the high-risk and low-risk groups

Microbial communities tend to influence each other; thus, we analyzed the network of co-expression relationships between different microbiomes at the genus level to understand the overall changes between the high-risk and low-risk groups. The results showed that the co-expression networks of the microbiota significantly differed between the two groups. Interestingly, we performed both positive and negative correlation analyses, but only the positive correlation networks showed statistical significance for reasons that require further research.

A closely related module appeared in the co-expression network of both the high-risk and low-risk groups; however, the co-expression networks were completely different. The high-risk modules included *Oleomonas*, *Cellulomonas*, *Rhodopirellula*, *Cycloclasticus*, *Candidatus Paracaedibacter*, *Prosthecobacter*, *Aphanizomenon*, and *Thiothrix* (Fig. 6A). After reviewing the literature, we found that studies on these bacterial genera are scarce, indicating the potential for further research in this direction.

The microorganisms in the module in the low-risk group were *Arthrospira*, *Candidatus Protochlamydia*, *Rheinheimera*, *Candidatus Vidania*, *Halobacteroides*, *Lebetimonas*, *Dictyoglomus*, *Formos*, *Thermodesulfobium*, *Anacrofu stis*, *Dactylococcopsis*, *Butyrivibrio*, *Mitsuokella*, *Nitratiruptor*, and *Brachyspira* (Fig. 6B). Interestingly, in the low-risk group module, *Butyrivibrio* and *Arthrospira* have been reported as microorganisms that are beneficial to human health. Previous studies have reported that better diet quality according to multiple healthy dietary patterns is associated with a greater abundance of *Butyrivibrio species*[24]. *Arthrospira* is a free-floating fine filamentous cyanobacteria. It is believed to have potential antioxidant, anti-inflammatory, immunomodulatory, weight loss and antitumor effects[25–27]. In general, the intratumoral microbiota in low-risk patients appears to be composed of beneficial microbial communities.

LEfSe analysis and construction of a novel microbial-based scoring (MS) system

To search for biomarkers of the microbiota in bladder cancer, LEfSe analysis was performed, and 41 vital microorganisms were ultimately identified (Fig. 7B). A detailed cladistic evolution diagram is shown in Fig. 7A.

Based on these 41 biomarkers, we conducted an analysis combining patient survival data and ultimately identified six key prognostic bacteria (Supplementary Table 9). Through LASSO regression analysis, we established a new MS system composed of *Syntrophobotulus*, *Granulicatella*, *Xanthomonas*, Aquificae, *Niabella*, and *Pseudoalteromonas* (Fig. 7C-D, Supplementary Table 10). We used this MS system to score the BLCA patients. However, some BLCA patients found none of the key bacteria in the MS system, so they scored 0 and were labeled as the MS-0 group. The rest of the patients were labeled as either the MS- group or the MS+ group, based on their positive or negative scores (Supplementary Table 11). The K-M survival curve showed the prognosis of the three groups (Fig. 7E). The prognosis of patients in the MS-0 group was different from that in the MS + group, but there was no statistical difference compared with that in the MS- group. Therefore, we decided to merge the MS-0 group with the MS- group to form the MS-Low group (patients in this group lack tumor-promoting intratumoral microbiota), while the MS + group was designated as the MS-High group. The

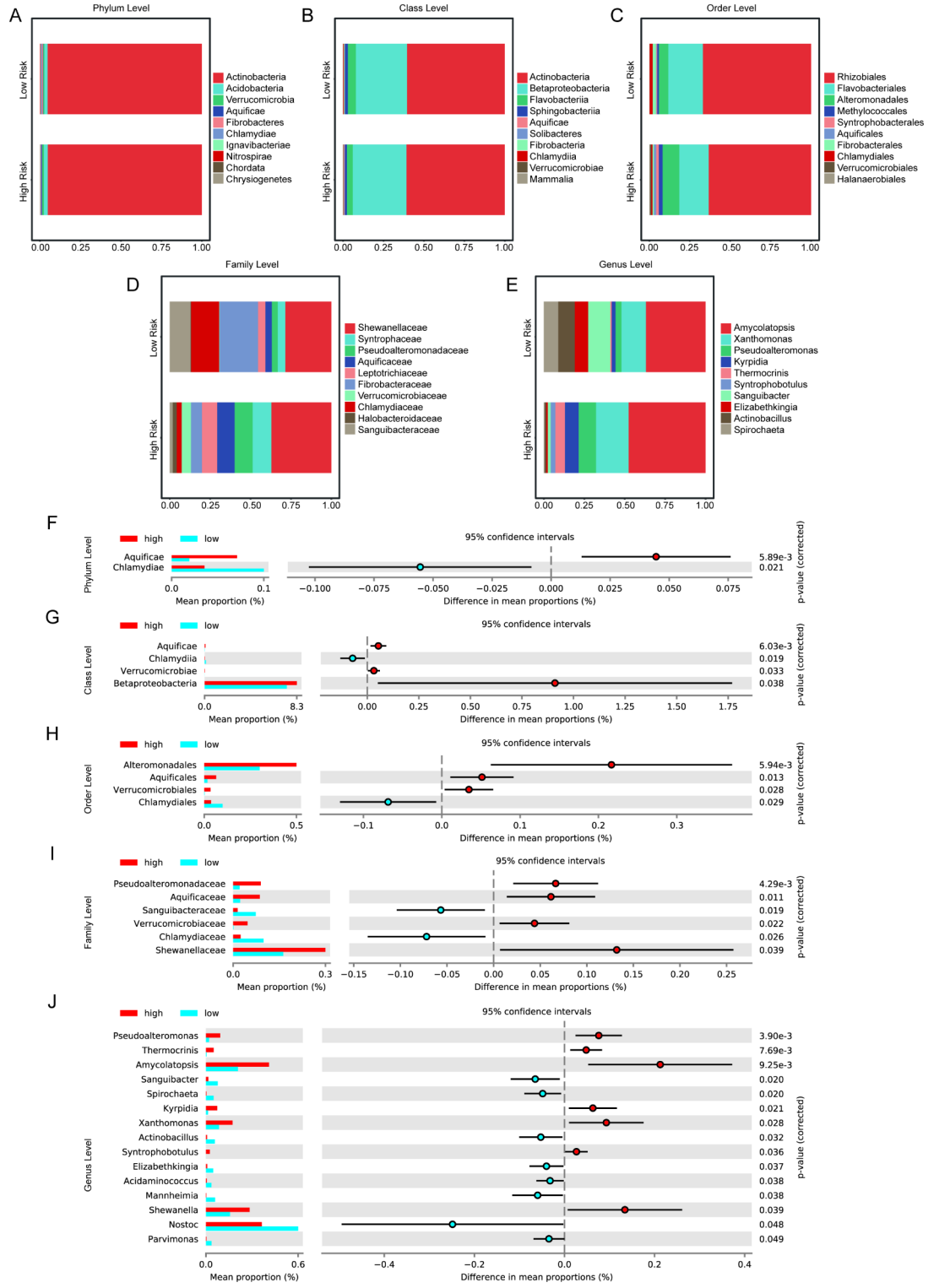

Fig. 5. Microbiota composition and STAMP analysis at various taxonomic levels in the high-risk and low-risk groups. (**A**-**E**) Stacked bar charts show that the bacterial composition of the two groups is quite different at the level of family and genus. (**F**-**J**) Forest plot displaying the results of STAMP analysis at various taxonomic levels in the two groups.

K-M survival curve showed the differential prognosis of the two groups (Fig. 7F). We also compared the clinical characteristics of the two groups of patients, including age, gender, grade, stage, race, etc., but there was no statistical difference (Supplementary Table 12). To date, we have identified the hub microbiota within the tumors of BLCA patients, and the novel MS system constructed from this information can subgroup patients.

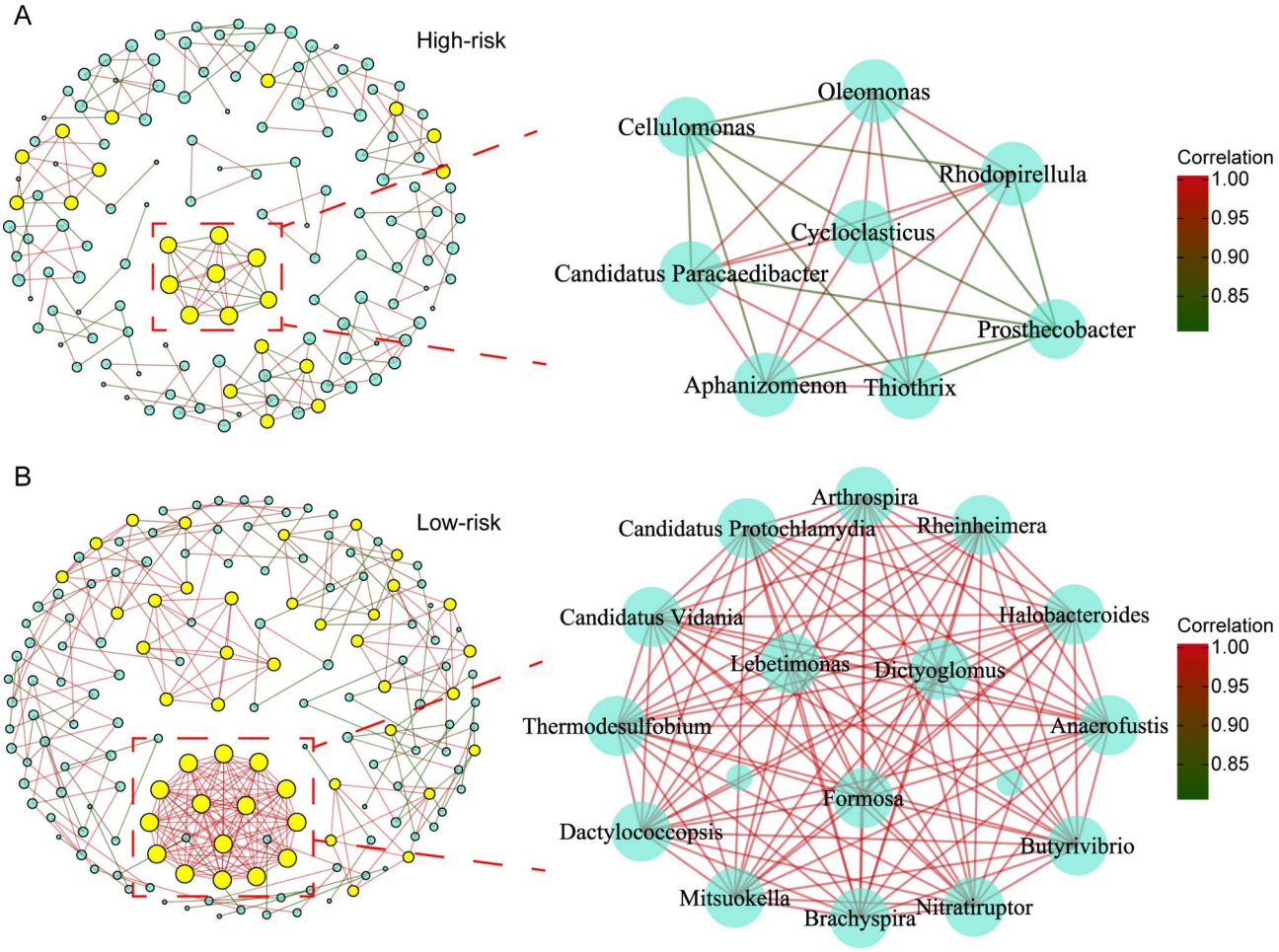

Fig. 6. Microbiota co-expression network in the high-risk and low-risk groups. (**A**) Network showing the microbiota co-expression relationships in the high-risk groups. (**B**) Network showing the microbiota co-expression relationships in the low-risk group. The size of the dot represents the relative abundance of bacteria, while the color of the dot represents its status in the network. The blue dots represent general points, while the yellow dots represent pivotal points in the network that are co-expressed with at least four other dots.

In addition, we analyzed the relative abundance of these six microorganisms and their clinical relevance to patients. The K-M plots revealed that a high abundance of *Syntrophobotulus*, *Granulicatella*, *Xanthomonas*, and *Pseudoalteromonas* was associated with worse patient outcomes (Supplementary Fig. 4A-F). Although the K-M map of *Niabella* was not significantly different, a greater abundance of Niabella appeared to be associated with longer OS. Interestingly, we found that Aquificae were significantly more abundant in stage 1 patients, suggesting that intratumoral bacteria may be related to clinical stage (Supplementary Fig. 4G). We analyzed the relative abundance of microorganisms involved in the MS system in the BIC database, and only the Aquificae class showed significant differences between different races (Supplementary Fig. 4H), while the relative abundance of all other microorganisms showed no significant differences between different races.

Immune cell infiltration characteristics in distinct MS subgroups

To further investigate the relationship between microorganisms in bladder cancer and tumor immunity, we calculated the infiltration of 22 types of immune cells in different MS groups using CIBERSORT. The results showed that the expression of B cells memory was significantly greater in the MS-high group than in the MS-low group (Fig. 8A).

In addition, we analyzed the tumor mutation burden (TMB) of patients in different MS groups. Overall, patients in the low MS group had a greater TMB (90.68%) than those in the high MS group (85.06%). We then selected the ten genes with the highest mutation rates for visual analysis (Fig. 8B,C). It is clear that the most frequently mutated genes of patients in different MS groups are significantly different. For example, the mutation rates of *TP53* and *KDM6A* are 6% and 7% greater, respectively, in MS-Low patients than in MS-High patients. Conversely, the mutation rate of *SYNE1* is 5% lower in MS-Low patients than in MS-High patients. Whether the different mutations of these genes are related to the different prognosis of bladder cancer patients is worthy of further study.

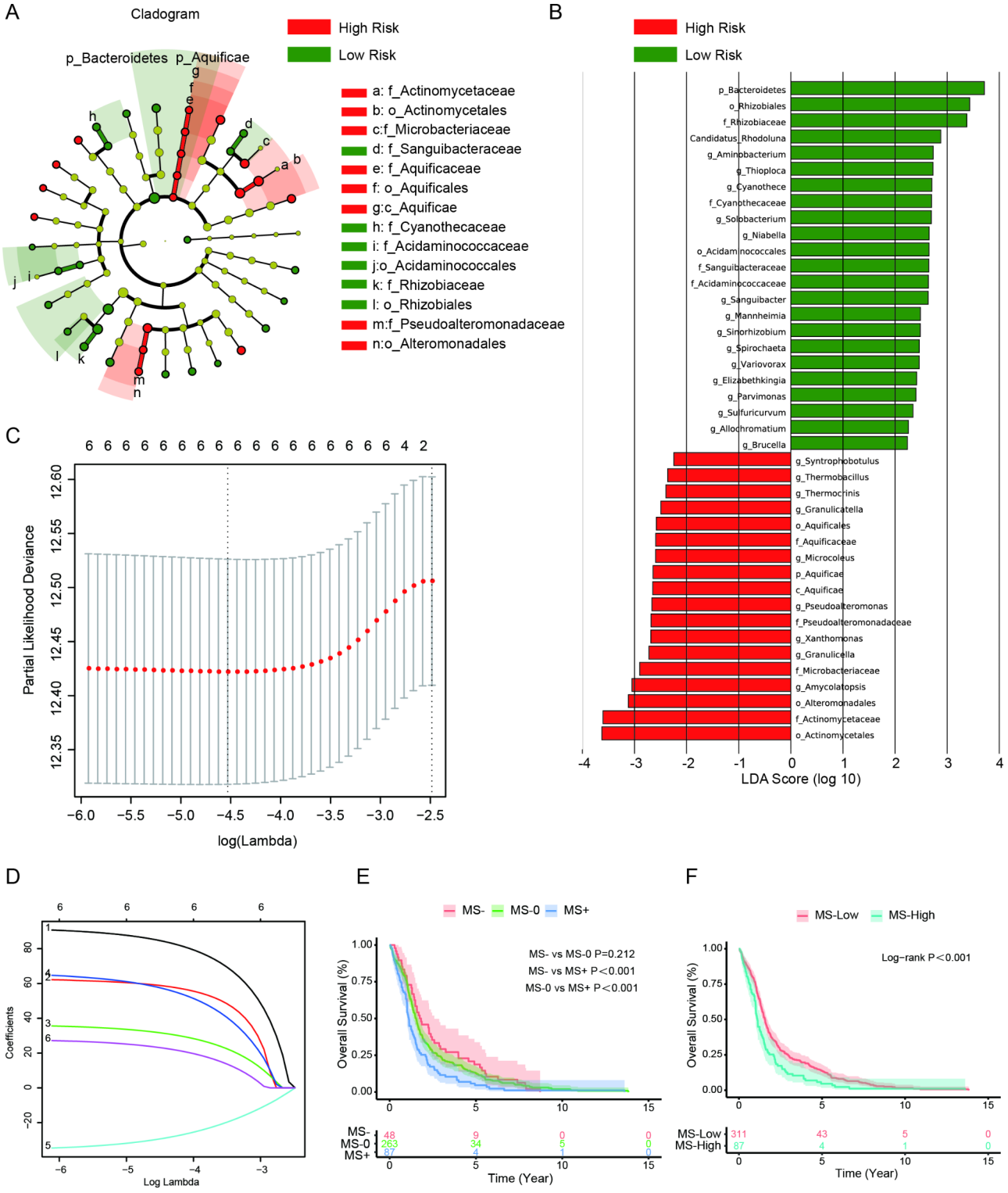

Fig. 7. LEfSe analysis and construction of a novel MS system. (**A**) The cladogram displays bacterial biomarkers that exhibit significant differences between the high-risk and low-risk groups. The colors of the nodes are as follows: yellow for species with no significant differences and red and green for microbial taxa that play a crucial role in the indicated groups. The names of the biomarkers that could not be fully displayed in the cladogram are shown on the right side. (**B**) Linear discriminant analysis (LDA) score of distinct bacteria in the high-risk and low-risk groups. (**C**, **D**) LASSO Cox regression analysis of distinct bacteria based on LEfSe analysis. (**E**) K-M plot of the three groups based on MS data. (**F**) The overall survival of BLCA patients in the MS-low group was longer than that in the MS-high group.

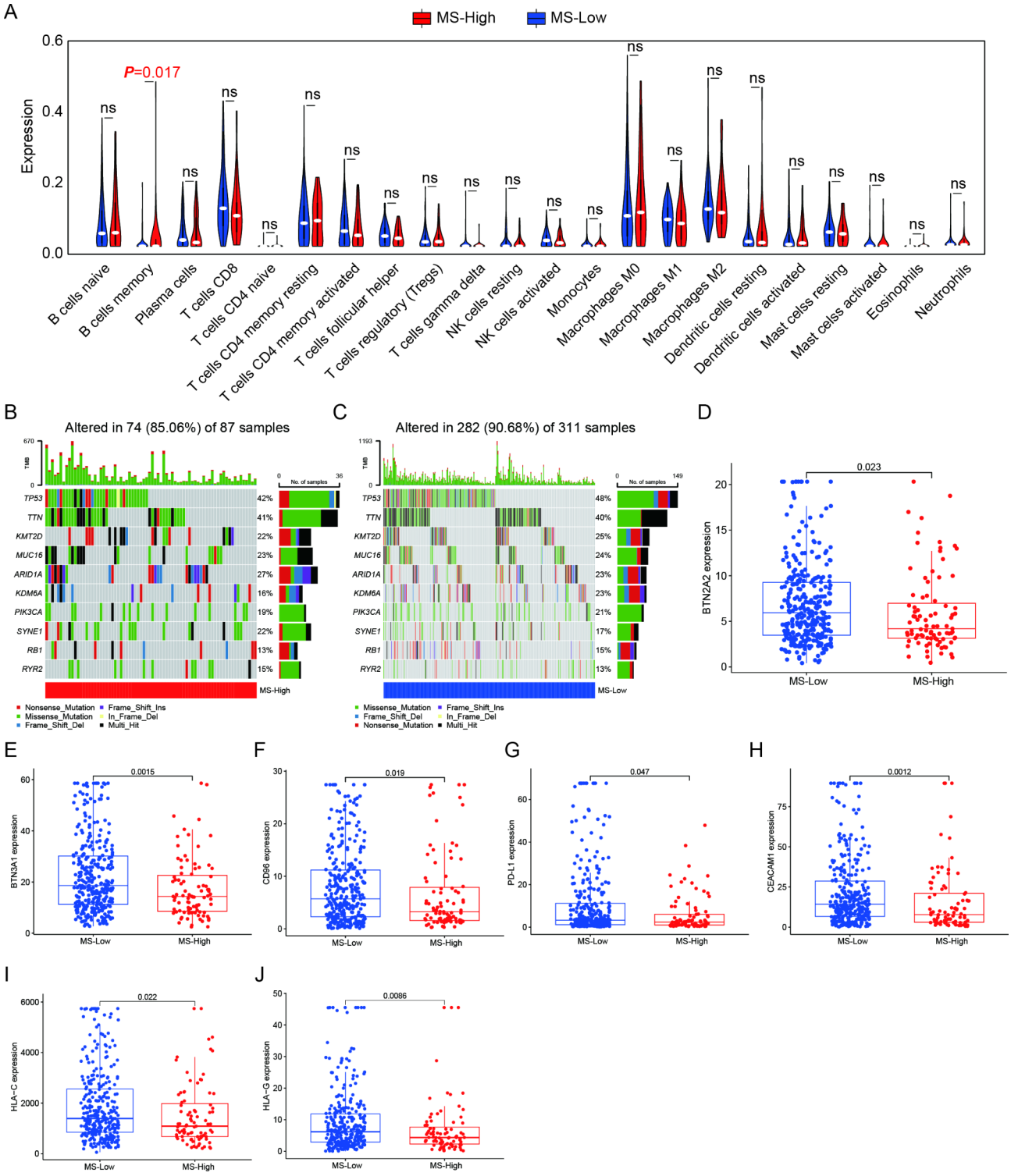

Fig. 8. Analyses of tumor immunity and the MS system. (**A**) Differences in immune cell infiltration between the MS-High and MS-Low groups. (**B**, **C**) Oncoplot showing the top 10 genes with the highest mutation rates in the MS-High and MS-Low groups. (**D**-**J**) The differential expression of immune checkpoints in the MS-High and MS-Low groups.

Finally, referring to the previous study[28], we compared the differential expression of several important ICI between the high- and low-MS groups. Results can be seen in Supplementary Table 13. The results showed that expression of BTN2A2, BTN3A1, CD96, PD-L1, CEACAM1, HLA-C, and HLA-G was significantly increased in patients with low MS (Fig. 8D-J).

Discussion

The human body harbors a rich diversity of microorganisms, among which the gut microbiota is one of the most important and closely related to human health[29]. Recent research has revealed that microorganisms also exist in many other tissues of the body, and significant differences are present in the microbial structures among different tissues. For instance, disruptions in the microbial ecosystem of tissues such as the skin and oral cavity have been closely associated with diseases[30,31]. Recent groundbreaking discoveries indicate that tumors also harbor diverse microbial communities[32].

In normal tissues, the presence of microorganisms is relatively low due to surveillance and clearance by the immune system. However, microorganisms within tumor tissues can exploit the immune evasion properties of tumor cells and proliferate abundantly. In particular, in the central necrotic areas of solid tumors, the abundance of microorganisms is much greater than that in surrounding normal tissues[33]. The microbial community within tumors is protected by the tumor and to some extent, can influence tumor progression. For example, the microbial community within tumors can promote the metastasis and colonization of breast cancer[6]. Immune cells infiltrating the tumor microenvironment can regulate tumors and impact patient prognosis. Therefore, reshaping the tumor immune microenvironment by targeting microorganisms within tumors is a promising strategy for enhancing antitumor immune responses.

With the advancement of detection techniques, urine is no longer considered sterile[34], raising questions about the presence of a microbiota in the urogenital system tissues that are constantly exposed to urine. The concept of the urine microbiota has great potential for studying the microbial composition within urogenital tumors. Kidney, bladder, and prostate cancers are three types of urogenital tumors that pose serious threats to human health, with bladder cancer being the most common malignancy among male urogenital tumors[35]. Therefore, studying the microbiota within bladder cancer is highly important. Currently, the characteristics of the tumor microbiota within bladder cancer and its role in the development, prognosis, and treatment of bladder cancer remain unclear.

Dohlman et al. and Poore et al. obtained bacterial expression profiles from RNA-sequencing (seq), whole-genome sequencing (WGS), and whole-exon sequencing (WXS) in the TCGA database[36,37]. However, they overlooked significant small-RNA seq data. In fact, there are distinct advantages to utilizing miRNA-seq over WGS, WXS, and RNA-seq. First, small RNAs have been shown to play a regulatory role in bacterial infections and bacterial infectious diseases. Second, in numerous RNA-seq investigations, RNA was extracted and reverse-transcribed into cDNA via the poly-A tail, leading to the exclusion of most bacterial RNAs lacking poly-A tails in the RNA-seq data. In contrast, miRNA-seq, which is conducted without poly-A filtration, offers the opportunity to detect bacteria that may not be captured by RNA-seq[21]. For the first time, in the BIC database, TCGA miRNA sequencing data were used to analyze the bacterial abundance and transcriptional pattern of 32 cancers. Consequently, the BIC database serves as a valuable complement to the sequencing data within TCGA and is ideally suited for analyzing the transcriptional landscape of bacteria in cancer.

In the present study, we conducted a comprehensive analysis of the intratumoral microbiota of bladder cancer patients with the help of the BIC database and identified six key microorganisms. Based on these findings, we developed a novel MS system that can effectively predict patient prognosis. Overall, these results provide new research directions for studying the interaction between the immune microenvironment and intratumorl microbiota in bladder cancer.

Our FISH results suggest that the abundance of microbiota in bladder cancer tissues is much greater than that in normal bladder tissues, suggesting the potential importance of the intratumoral microbiota. We conducted an analysis of the bacterial diversity across cancers in the BIC database, and the results showed that bladder cancer exhibited relatively high microbial diversity. The complex microbiome structure in bladder cancer led us to consider whether it has similarities with other tumors. First, we compared the microbial community structure in bladder cancer patients with that in COAD and READ patients, and significant differences were observed. Subsequently, we compared the microbial community structures within three types of urogenital tumors. Interestingly, the three tumors exhibited similar microbial community structures. This similarity raises the question of whether a correlation exists with urine microbiota, which requires further in-depth research.

The relationship between the intratumoral microbiota and tumor immunity is highly complex. Different intratumoral microbial ecosystems may lead to different tumor subtypes and result in distinct prognostic outcomes. In contrast to previous studies focusing on cancer and adjacent normal tissues, our research focused on the impact of the intratumoral microbiota on tumor malignancy progression. We downloaded lists of antimicrobial-related genes and tumor immunity-related genes from the TISIDB and ImmPort databases and integrated them with the bladder cancer dataset from TCGA. Through this analysis, we identified 331 DEIARGs in bladder cancer. By incorporating patient survival information, we ultimately identified 11 hub genes, including the important immune checkpoint PD-L1[38]. Based on these 11 hub genes, we constructed a microbial-tumor immune-related prognostic model and successfully stratified bladder cancer patients into high-risk and low-risk groups. Both K-M plots and ROC curves demonstrated the reliability of our model.

Furthermore, we conducted a comprehensive analysis of the intratumoral microbiota of bladder cancer patients in the high-risk and low-risk groups. We observed distinct differences in microbial community structures at the phylum and genus levels. For instance, at the genus level, the abundances of *Thermocrinis* and *Syntrophobotulus* were significantly lower in the low-risk group. However, these two bacteria are still understudied. Subsequent STAMP analysis also revealed microbial differences at different levels between the two groups.

Intratumoral microbiota do not exist in isolation but rather as a microbial community. Therefore, we analyzed the co-expression of microbiota in both groups. Interestingly, only the positively correlated microbial networks showed statistical significance. The results indicate that bladder cancer patients from the high-risk and low-risk groups have completely different co-expression networks of the intratumoral microbiota. Specifically, in the modules of the low-risk group, *Butyrivibrio* and *Arthrospira* were reported to be beneficial bacteria for

human health[24,26]. Most of the bacteria in the network have not been extensively studied in relation to tumors, highlighting the need for further research.

Previous studies have reported that certain intratumoral microbiota of human tumors may also be potential biomarkers for survival outcomes and immunotherapy[39,40]. To identify the crucial microbiota in bladder cancer, we conducted LEfSe analysis on the two groups and developed a novel MS system. Based on the MS system, we classified TCGA bladder cancer patients into MS-high and MS-low groups. Survival analysis revealed significant differences in prognosis between the two groups of patients. Ultimately, we identified six hub microbiota in bladder cancer that can define different tumor subtypes and lead to distinct prognostic outcomes.

Several studies have shown that the microbiome mediates the host immune system through a synergistic mechanism[41]. For instance, *Clostridium butyricum* and its metabolite butyrate were reported to promote ferroptosis susceptibility in pancreatic ductal adenocarcinoma[42]. To further investigate the relationship between the intratumoral microbiota and tumor immunity in bladder cancer, we utilized the CIBERSORT algorithm to reveal differences in 22 infiltrating immune cells between the MS-high and MS-low groups. Interestingly, we found a significant enrichment of B cells memory in the MS-high group. Additionally, our study also revealed significant differences in the TMB between different MS groups in patients with bladder cancer. We observed a considerable diversity of gene mutations between the MS-high and MS-low groups, suggesting that the intratumoral microbiota may simultaneously influence the tumor genomic landscape.

Research on urinary microbiota is currently limited, and even fewer studies have focused on the intratumoral microbiota in the urogenital system. In contrast to previous studies, this study primarily explored the grouping of bladder cancer subtypes based on intratumoral microbiota. We investigated the potential relationship between intratumoral microbiota and tumor immunity in patients with bladder cancer. However, this study has certain limitations. It is based on bioinformatics analysis of the TCGA dataset, primarily focusing on MIBC patients. Whether this conclusion holds true in NMIBC patients remains unknown. Therefore, to further validate the findings of this study, relevant in vitro and in vivo experiments are essential.

The intratumoral microbiota of bladder cancer can be considered a novel target for tumor diagnosis, prognosis, and treatment. As a significant component of the tumor microenvironment, research on the intratumoral microbiota of bladder cancer holds great significance and broad application prospects. For instance, drugs targeting key intratumoral microbiota may effectively treat bladder cancer patients. However, it is worth noting that not all intratumoral microbiota promote malignant tumor progression; some seem to exhibit tumor-suppressive properties. This suggests the need for more precise selection of microbial targets for drug therapy rather than broad-spectrum antimicrobial approaches.

In this study, we identified six key bladder cancer biomarkers and developed a novel MS system. This model allows for the subtyping of bladder cancer patients, showing different prognostic outcomes and immune checkpoint profiles across different scoring groups. Future research can involve a series of in vivo and in vitro experiments focusing on the intratumoral microbiota involved in this MS system.

We hope that our study will contribute to a better understanding of the intratumoral microbiota of bladder cancer and provide insights for future research.

Materials and methods

Data acquisition

The transcriptome profile, clinical data, and simple nucleotide variation data were obtained from The Cancer Genome Atlas (TCGA) database (https://portal.gdc.cancer.gov/) on July 27, 2023. The dataset included 412 bladder cancer samples and 19 normal samples. The antimicrobial-related gene list was obtained from the Immunology Database and Analysis Portal (ImmPort) database (https://www.immport.org/), while the antitumor immunity-related gene list was obtained from the TISIDB (http://cis.hku.hk/TISIDB/index.php). Additionally, we obtained microbial profiles at the phylum, class, order, family, and genus levels for the 412 bladder cancer samples from the Bacteria in Cancer (BIC) database (http://bic.jhlab.tw/).

Ethics statement and sample acquisition

The bladder cancer tissues and adjacent normal tissues used in the present study were obtained from the Specimen Bank of the Department of Urology, Jiangnan University Medical Center. None of the bladder cancer patients had other tumors. All samples were obtained in a sterile operating room and subsequently frozen and stored at -80 °C. This study was approved by the Ethics Committee of the Jiangnan University Medical Center (2023-Y-167). All methods were carried out in accordance with relevant guidelines and regulations. Informed consent was obtained from all subjects and/or their legal guardian(s).

Fluorescence in situ hybridization (FISH) and immunofluorescence (IF)

Freshly frozen tissues were fixed in 4% paraformaldehyde for 24 h, followed by gradient dehydration in alcohol and embedding in paraffin. The paraffin-embedded tissues were then sliced into slides. The slides were incubated at 37 °C in prehybridization solution for 30 min. Next, hybridization solution containing the FISH probe EUB338 (5′-GCT GCC TCC CGT AGG AGT-3′) specific for bacterial 16 S rRNA was added. The samples were incubated overnight at 37 °C in a humid environment. After FISH, IF experiments were performed. First, the hybridization solution was removed, and then the slides were incubated overnight at 4 °C with the indicated primary antibodies (anti-CD8: Proteintech #66868-1-Ig, anti-CD68: Proteintech #66231-2-Ig, anti-CD86: ABCAM #ab220188, and anti-CD206: Proteintech #60143-1-Ig). Subsequently, the slides were incubated with fluorescently labeled secondary antibodies at room temperature for 1 h. Nuclear staining was performed using 4′,6-diamidino-2-phenylindole (DAPI) at room temperature. Finally, images were captured under a fluorescence microscope (OLYMPUS BX53, Tokyo).

Online analysis
The BIC database contains data on intratumoral bacterial diversity and composition across cancers. Using Venn diagrams generated by Jvenn (https://jvenn.toulouse.inrae.fr/app/index.html), an online tool, we compared BLCA with other tumors.

Identification of differentially expressed immune- and antimicrobial-related genes (IARGs)
The list of IARGs was obtained from the ImmPort and TISIDB databases. The transcriptomic profiles of BLCA patients were analyzed using the "Limma" package in R software (version 4.3.1) with the criteria of a false discovery rate < 0.05 and a |log2-fold change| > 1. A total of 4,840 genes were differentially expressed between BLCA patient tissues and normal tissues. The results overlapped with the list of IARGs, and the intersecting genes were considered differentially expressed IARGs (DEIARGs) in BLCA.

Identification of hub DEIARGs through univariate, multivariate and LASSO Cox regression analyses
Considering the complexity of prognosis, different studies have used different statistical methods to construct prognostic models[43–45]. However, least absolute shrinkage and selection operator (LASSO) regression and univariate and multivariate Cox regression were more suitable for model construction in this study[46]. Univariate Cox regression analysis was initially conducted to identify prognosis-related DEIARGs. Subsequently, LASSO Cox regression analysis was performed to identify genes with the least error. Finally, multivariate Cox regression analysis was carried out, and the genes identified were considered hub genes.

Construction of the DEIARG-based prognostic risk model
A prognostic index based on the DEIARGs was constructed using the mRNA expression levels of the hub genes. These expression levels were weighted by the estimated regression coefficient obtained from the multivariate Cox regression model. The index is calculated as the product of the coefficient (coef i) and the expression level (Expr i) of each DEIARG for patient i.

To evaluate the effectiveness of the prognostic risk model, we randomly assigned TCGA patients to two groups: the training group ($n = 269$) and the testing group ($n = 132$). All patients were further divided into high-risk and low-risk groups based on the median risk score obtained from the training group. K-M survival curves were constructed to assess whether the index was a prognostic factor for OS. Additionally, receiver operating characteristic (ROC) curves were generated to validate the DEIARG-based model.

Microbiota diversity analysis of the high-risk and low-risk groups
The alpha and beta diversity of intratumoral bacteria between the high-risk and low-risk groups was calculated using the "picante" and "vegan" packages of R software, utilizing microbial abundance data obtained from the BIC database. All analyses were performed at the phylum and genus levels.

Microbiota abundance analysis of the high-risk and low-risk groups
First, we analyzed the relative abundance of microbiota at the phylum, class, order, family, and genus levels for the high-risk and low-risk groups. Next, we performed statistical analysis of metagenomic profiles (STAMP) on the data from the BIC database to investigate the overall differences in microbial community profiles between the high-risk and low-risk groups.

Construction of bacterial co-expression networks in the high-risk and low-risk groups
We used the "Hmisc" package of R software to conduct correlation analysis of intratumoral bacteria in the high-risk and low-risk groups. The "ggraph" package was used to construct the plots.

LEfSe analysis in the high-risk and low-risk groups
To determine the differences in the microbiota between the high-risk and low-risk groups, we used LEfSe software to identify potential biomarkers. The statistical analysis of differences was combined with scores for the influence of the species on the grouping outcomes while emphasizing statistical significance and biological correlations.

Generation of a novel microbial-based scoring (MS) system
Based on the expression of potential biomarkers determined by LEfSe analysis in the BIC database combined with clinical information, we identified six hub bacteria through univariate Cox regression analysis. Furthermore, we performed LASSO regression analysis and finally established a novel MS system. The score of the index = (LassoCoef i $*$ Expr i), where LassoCoef i was the lasso coefficient of the hub bacteria i and Expr i was the expression of the hub bacteria for patient i.

All bladder cancer patients were divided into MS-, MS-0 and MS + groups according to the MS score. We combined the MS-0 group with the MS- group as the MS-Low group. The MS + group was designated as the MS-High group. A K-M survival plot was constructed to assess whether this index could be a prognostic indicator for overall survival.

Analyses of tumor immunity and the MS system
The "Immunedeconv" package of R software was used to analyze CIBERSORT immune infiltration. The overall mutation landscape and immune checkpoint genes were summarized through the "Limma" package. In addition, the "ggplot2" and "ggpubr" packages were utilized to construct the plots.

Statistical analysis

Analyses were performed with the aid of R software (version 4.3.1). The independent t test was used to compare normally distributed continuous variables, while the Mann-Whitney U test was used to compare skewed continuous variables. All statistical *P* values were two-sided, with $P < 0.05$ indicating statistical significance.

Data availability

The data of the present study are available from the corresponding author on reasonable request.

Received: 22 June 2024; Accepted: 11 September 2024
Published online: 27 September 2024

References

1. Qian, X. B. et al. A guide to human microbiome research: Study design, sample collection, and bioinformatics analysis. *Chin. Med. J. (Engl.)* **133**, 1844–1855. https://doi.org/10.1097/CM9.0000000000000871 (2020).
2. Quevrain, E. et al. Identification of an anti-inflammatory protein from *Faecalibacterium prausnitzii*, a commensal bacterium deficient in Crohn's disease. *Gut*. **65**, 415–425. https://doi.org/10.1136/gutjnl-2014-307649 (2016).
3. Wilson, M. R. et al. The human gut bacterial genotoxin colibactin alkylates DNA. *Science*. https://doi.org/10.1126/science.aar7785 (2019).
4. Geller, L. T. et al. Potential role of intratumor bacteria in mediating tumor resistance to the chemotherapeutic drug gemcitabine. *Science*. **357**, 1156–1160. https://doi.org/10.1126/science.aah5043 (2017).
5. Knippel, R. J., Drewes, J. L. & Sears, C. L. The cancer microbiome: Recent highlights and knowledge gaps. *Cancer Discov.* **11**, 2378–2395. https://doi.org/10.1158/2159-8290.CD-21-0324 (2021).
6. Fu, A. et al. Tumor-resident intracellular microbiota promotes metastatic colonization in breast cancer. *Cell* 185, 1356–1372 e1326 (2022). https://doi.org/10.1016/j.cell.2022.02.027
7. Walker, S. P., Tangney, M. & Claesson, M. J. Sequence-based characterization of intratumoral bacteria—a guide to best practice. *Front. Oncol.* **10**, 179. https://doi.org/10.3389/fonc.2020.00179 (2020).
8. Gur, C. et al. Binding of the Fap2 protein of *Fusobacterium nucleatum* to human inhibitory receptor TIGIT protects tumors from immune cell attack. *Immunity*. **42**, 344–355. https://doi.org/10.1016/j.immuni.2015.01.010 (2015).
9. Nejman, D. et al. The human tumor microbiome is composed of tumor type-specific intracellular bacteria. *Science*. **368**, 973–980. https://doi.org/10.1126/science.aay9189 (2020).
10. Allen-Vercoe, E., & Coburn, B. A microbiota-derived metabolite augments cancer immunotherapy responses in mice. *Cancer Cell* **38**, 452–453. https://doi.org/10.1016/j.ccell.2020.09.005 (2020).
11. Zagato, E. et al. Endogenous murine microbiota member *Faecalibaculum rodentium* and its human homologue protect from intestinal tumour growth. *Nat. Microbiol.* **5**, 511–524. https://doi.org/10.1038/s41564-019-0649-5 (2020).
12. Mager, L. F. et al. Microbiome-derived inosine modulates response to checkpoint inhibitor immunotherapy. *Science*. **369**, 1481–1489. https://doi.org/10.1126/science.abc3421 (2020).
13. Riquelme, E. et al. Tumor microbiome diversity and composition influence pancreatic cancer outcomes. *Cell* 178, 795–806 e712 (2019). https://doi.org/10.1016/j.cell.2019.07.008
14. Eklof, V. et al. Cancer-associated fecal microbial markers in colorectal cancer detection. *Int. J. Cancer*. **141**, 2528–2536. https://doi.org/10.1002/ijc.31011 (2017).
15. Gagniere, J. et al. Interactions between microsatellite instability and human gut colonization by *Escherichia coli* in colorectal cancer. *Clin. Sci. (Lond.)*. **131**, 471–485. https://doi.org/10.1042/CS20160876 (2017).
16. Lee, J. A. et al. Differential immune microenvironmental features of microsatellite-unstable colorectal cancers according to *Fusobacterium nucleatum* status. *Cancer Immunol. Immunother*. **70**, 47–59. https://doi.org/10.1007/s00262-020-02657-x (2021).
17. Siegel, R. L., Miller, K. D., Wagle, N. S. & Jemal, A. Cancer statistics, 2023. *CA Cancer J. Clin.* **73**, 17–48. https://doi.org/10.3322/caac.21763 (2023).
18. Dyrskjot, L. et al. Bladder cancer. *Nat. Rev. Dis. Primers*. **9**, 58. https://doi.org/10.1038/s41572-023-00468-9 (2023).
19. Gram, I. T., Sandin, S., Braaten, T., Lund, E. & Weiderpass, E. The hazards of death by smoking in middle-aged women. *Eur. J. Epidemiol.* **28**, 799–806. https://doi.org/10.1007/s10654-013-9851-6 (2013).
20. Bi, H. et al. Urinary microbiota—A potential biomarker and therapeutic target for bladder cancer. *J. Med. Microbiol.* **68**, 1471–1478. https://doi.org/10.1099/jmm.0.001058 (2019).
21. Chen, K. P., Hsu, C. L., Oyang, Y. J., Huang, H. C. & Juan, H. F. BIC: A database for the transcriptional landscape of bacteria in cancer. *Nucleic Acids Res.* **51**, D1205–D1211. https://doi.org/10.1093/nar/gkac891 (2023).
22. Li, W. et al. Correlation between PD-1/PD-L1 expression and polarization in tumor-associated macrophages: A key player in tumor immunotherapy. *Cytokine Growth Factor. Rev.* **67**, 49–57. https://doi.org/10.1016/j.cytogfr.2022.07.004 (2022).
23. Kanehisa, M. & Goto, S. KEGG: Kyoto encyclopedia of genes and genomes. *Nucleic Acids Res.* **28**, 27–30. https://doi.org/10.1093/nar/28.1.27 (2000).
24. Peters, B. A. et al. Healthy dietary patterns are associated with the gut microbiome in the Hispanic Community Health Study/Study of latinos. *Am. J. Clin. Nutr.* **117**, 540–552. https://doi.org/10.1016/j.ajcnut.2022.11.020 (2023).
25. Naeini, F. et al. Spirulina supplementation as an adjuvant therapy in enhancement of antioxidant capacity: A systematic review and meta-analysis of controlled clinical trials. *Int. J. Clin. Pract.* **75**, e14618. https://doi.org/10.1111/ijcp.14618 (2021).
26. Sorrenti, V. et al. Spirulina microalgae and brain health: A scoping review of experimental and clinical evidence. *Mar. Drugs*. https://doi.org/10.3390/md19060293 (2021).
27. Moradi, S. et al. Effects of Spirulina supplementation on obesity: A systematic review and meta-analysis of randomized clinical trials. *Complement. Ther. Med.* **47**, 102211. https://doi.org/10.1016/j.ctim.2019.102211 (2019).
28. Zhang, Y. et al. Construction and verification of a prognostic risk model based on immunogenomic landscape analysis of bladder caner. *Gene*. **808**, 145966. https://doi.org/10.1016/j.gene.2021.145966 (2022).
29. Joachim, L. et al. The microbial metabolite desaminotyrosine enhances T-cell priming and cancer immunotherapy with immune checkpoint inhibitors. *EBioMedicine*. **97**, 104834. https://doi.org/10.1016/j.ebiom.2023.104834 (2023).
30. Farias Amorim, C. et al. Multiomic profiling of cutaneous leishmaniasis infections reveals microbiota-driven mechanisms underlying disease severity. *Sci. Transl Med.* **15**, eadh1469. https://doi.org/10.1126/scitranslmed.adh1469 (2023).
31. Huang, L. et al. The role of the microbiota in glaucoma. *Mol. Aspects Med.* **94**, 101221. https://doi.org/10.1016/j.mam.2023.101221 (2023).
32. Sepich-Poore, G. D. et al. The microbiome and human cancer. *Science*. https://doi.org/10.1126/science.abc4552 (2021).
33. McAllister, F., Khan, M. A. W., Helmink, B. & Wargo, J. A. The tumor microbiome in pancreatic cancer: Bacteria and beyond. *Cancer Cell* **36**, 577–579 (2019).
34. Miller, A. W. et al. Mechanisms of the intestinal and urinary microbiome in kidney stone disease. *Nat. Rev. Urol.* **19**, 695–707. https://doi.org/10.1038/s41585-022-00647-5 (2022).

35. Jubber, I. et al. Epidemiology of bladder Cancer in 2023: A systematic review of risk factors. *Eur. Urol.* **84**, 176–190. https://doi.org/10.1016/j.eururo.2023.03.029 (2023).
36. Dohlman, A. B. et al. The cancer microbiome atlas: A pan-cancer comparative analysis to distinguish tissue-resident microbiota from contaminants. *Cell Host Microbe* 29, 281–298 e285 (2021). https://doi.org/10.1016/j.chom.2020.12.001
37. Poore, G. D. et al. Microbiome analyses of blood and tissues suggest cancer diagnostic approach. *Nature*. **579**, 567–574. https://doi.org/10.1038/s41586-020-2095-1 (2020).
38. Roupret, M. et al. European Association of Urology Guidelines on Upper urinary tract urothelial carcinoma: 2023 update. *Eur. Urol.* **84**, 49–64. https://doi.org/10.1016/j.eururo.2023.03.013 (2023).
39. Van der Merwe, M., Van Niekerk, G., Botha, A. & Engelbrecht, A. M. The onco-immunological implications of *Fusobacterium nucleatum* in breast cancer. *Immunol. Lett.* **232**, 60–66. https://doi.org/10.1016/j.imlet.2021.02.007 (2021).
40. Sun, L. et al. Intratumoural microbiome can predict the prognosis of hepatocellular carcinoma after surgery. *Clin. Transl Med.* **13**, e1331. https://doi.org/10.1002/ctm2.1331 (2023).
41. Wong-Rolle, A., Wei, H. K., Zhao, C. & Jin, C. Unexpected guests in the tumor microenvironment: Microbiome in cancer. *Protein Cell.* **12**, 426–435. https://doi.org/10.1007/s13238-020-00813-8 (2021).
42. Yang, X. et al. *Clostridium butyricum* and its metabolite butyrate promote ferroptosis susceptibility in pancreatic ductal adenocarcinoma. *Cell. Oncol. (Dordr.)*. https://doi.org/10.1007/s13402-023-00831-8 (2023).
43. Li, X. Y. et al. m7G methylation-related genes as biomarkers for predicting overall survival outcomes for hepatocellular carcinoma. *Front. Bioeng. Biotechnol.* **10**, 849756. https://doi.org/10.3389/fbioe.2022.849756 (2022).
44. Zou, J. et al. A multi-omics-based investigation of the prognostic and immunological impact of necroptosis-related mRNA in patients with cervical squamous carcinoma and adenocarcinoma. *Sci. Rep.* **12**, 16773. https://doi.org/10.1038/s41598-022-20566-0 (2022).
45. Lin, Z. et al. Necroptosis-related lncRNA signature predicts prognosis and immune response for cervical squamous cell carcinoma and endocervical adenocarcinomas. *Sci. Rep.* **12**, 16285. https://doi.org/10.1038/s41598-022-20858-5 (2022).
46. Zhao, J. et al. Construction of N-7 methylguanine-related mRNA prognostic model in uterine corpus endometrial carcinoma based on multi-omics data and immune-related analysis. *Sci. Rep.* **12**, 18813. https://doi.org/10.1038/s41598-022-22879-6 (2022).

Acknowledgements

We are grateful to all the relevant online databases covered in the present study.

Author contributions

YW. Z.: Data curation, Formal analysis, Investigation, Methodology, Resources, Software, Writing–original draft, Writing–review & editing, Funding acquisition; H. L.: Data curation, Formal analysis, Resources, Software, Writing–original draft; LH. L.: Data curation, Formal analysis, Investigation, Resources, Software, Writing–original draft; SK. J.: Investigation, Resources, Writing–review & editing; J. L.: Investigation, Resources, Writing–review & editing; YH. Z.: Investigation, Resources, Writing–review & editing; F. X.: Data curation, Formal analysis, Project administration, Supervision, Validation, Visualization; FP. L.: Methodology, Project administration, Supervision, Visualization, Writing–review & editing; NH. F.: Funding acquisition, Methodology, Project administration, Resources, Supervision, Validation, Writing–review & editing.

Funding

This study was supported by the National Natural Science Foundation of China (82370777), and Postgraduate Research & Practice Innovation Program of Jiangsu Province (Item No: KYCX24_3596, SJCX23_0689).

Declarations

Competing interests

The authors declare no competing interests.

Additional information

Supplementary Information The online version contains supplementary material available at https://doi.org/10.1038/s41598-024-72918-7.

Correspondence and requests for materials should be addressed to F.X., F.L. or N.F.